Peroxynitrite Inactivation of Human Cytochrome P450s 2B6 and 2E1: Heme Modification and Site-Specific Nitrotyrosine Formation†

Hsia-lien Lin,‡ Eugene Myshkin,§ Lucy Waskell,§ and Paul F. Hollenberg*,‡

Department of Pharmacology, and Department of Anesthesiology, University of Michigan and VA Medical Center, Ann Arbor, Michigan 48109

Received June 20, 2007

This study examined the reaction of peroxynitrite (PN) with two human cytochrome P450s, P450 2B6 (2B6) and P450 2E1 (2E1). After the reaction with PN, the NADPH/reductase-supported 7-ethoxy-4-(trifluoromethyl)coumarin (EFC) deethylation activity of both P450s was decreased in a concentration-dependent manner. HPLC analysis revealed that the prosthetic heme group of 2B6 was modified but to a lesser extent than the decrease in enzymatic activity. In contrast, the heme moiety of 2E1 was not altered. These results suggest that protein modification by PN contributed to the loss in enzymatic activity of 2B6 and 2E1 but to different extents. After trypsin digestion of the control and PN-inactivated P450s, tyrosine nitration was used as a biomarker for protein modification and the addition of the nitro group was determined using electrospray ionization-liquid chromatography-tandem mass spectrometry, allowing site-specific assignment of the tyrosine residues nitrated. Tyrosine residues 354, 244, 268, and 380 in 2B6 and tyrosine residues 317, 422, 69, and 380 in 2E1 were found to be nitrated. Tyrosine 354 is the primary site of nitration in 2B6, and tyrosine residues 422 and 317 are the primary targets for nitration in 2E1. After PN exposure, the EFC catalytic activity of 2E1 supported by *tert*-butylhydroperoxide was not affected, and the activity of 2B6 supported by *tert*-butylhydroperoxide was decreased to a lesser extent than that supported by NADPH/reductase. Following exposure to PN, the levels of the reduced-CO complex were less than the content of native heme remaining. These results suggest that PN-mediated protein modification has no effect on substrate binding but may impair the interaction of the reductase with P450s, thereby inhibiting electron transfer. Homology modeling shows that Tyr422 of 2E1 is in close proximity to the FMN domain of reductase, suggesting that Tyr422 may be involved in transferring electrons from the reductase to the heme and thus may play a critical structural and functional role in the extensive activity loss following PN exposure.

Introduction

Peroxynitrite (PN)[1], a strong oxidant and nitrating agent capable of reacting with and modifying a wide variety of biomolecules including proteins, DNA, and lipids, is readily formed by the rapid reaction of nitric oxide and superoxide under pathophysiological conditions (*1–3*). A strong correlation between tyrosine nitration and the inactivation of protein function as a result of exposure to PN has been demonstrated for the abundance of proteins and in diverse diseases such as cerebral ischemia, chronic inflammatory processes, cardiovascular diseases, and neurodegenerative disorders (*2–5*). The formation of nitrotyrosine represents a specific PN-mediated protein modification; thus, the detection of nitrotyrosine in proteins is considered to be a biomarker for endogenous PN formation (*1–4*). PN-mediated damage may result in the modification of protein structure, metabolism, signal transduction, and may also promote adverse biological effects (*4–6*).

In humans and animals, the expression levels and activities of various forms of P450s in the liver as well as in extrahepatic tissue such as brain and kidney may be altered because of various infections or inflammatory stimuli (*7*). Nitric oxide synthesized by nitric oxide synthase during inflammatory episodes has been proposed to be responsible for the down regulation of hepatic P450 mRNA as well as the proteins (*8*). It has become apparent that a series of nitric oxide-dependent biological processes are not directly mediated by nitric oxide but rather that they depend on the formation of a secondary intermediate such as PN (*1, 3, 6*). Nitric oxide is produced in a variety of cells and may serve as a neurotransmitter, immunoregulator, and endothelium-derived relaxing factor (*1*). The NO synthases are heme proteins that share many structural and catalytic properties with P450s (*9*). Microsomal cytochrome P450s such as the P450 3A subfamily have also been implicated in the formation of nitric oxide from *N*-hydroxyarginine (*9*). Moreover, P450 2B6, 2C9, and 2C19 can metabolize serotonin to nitric oxide in the presence of catalase (*10*). Following enzymatic generation of superoxide as a result of uncoupling of mitchondrial electron transport, NADPH-oxidase activity, or uncoupled catalytic turnover of the microsomal P450s, the

† It is a great honor and a pleasure to contribute to this special issue of *Chemical Research in Toxicology* paying tribute to my long time friend and distinguished colleague Professor Larry Marnett on the occasion of his 60th birthday. I am delighted to join the other authors in congratulating him on his many achievements and contributions to research in toxicology and to express my best wishes to him.

* To whom correspondence should be addressed. Paul F. Hollenberg, Department of Pharmacology, 2301 MSRB III, 1150 West Medical Center Drive, Ann Arbor, MI 48109-0632. Phone: (734) 764-8166. Fax: (734) 763-5387. E-mail: phollen@umich.edu.

‡ Department of Pharmacology.

§ Department of Anesthesiology.

[1] Abbreviations: PN, peroxynitrite; EFC, 7-ethoxy-4-(trifluoromethyl)-coumarin; 2B6, human cytochrome P450 2B6; 2E1, human cytochrome P450 2E1; reductase, NADPH-cytochrome P450 reductase; tBHP, *tert*-butylhydroperoxide; ESI, electrospray ionization; LC-MS/MS, liquid chromatography-tandem mass spectrometry; TFA, trifluoroacetic acid.

10.1021/tx700220e CCC: $37.00
Published on Web 10/02/2007

reaction between nitric oxide and superoxide, which is almost diffusion-controlled, will generate PN (*6, 9*). PN is more reactive and more toxic than nitric oxide and diffuses rapidly and permeates membranes to attack proteins in other cells and cellular compartments (*3*). Therefore, it is highly likely that PN can be formed and accumulated in the vicinity of microsomal P450s. Thus, the P450s may be a source of PN as well as a target for PN-mediated oxidative damage (*9*).

In the past few years, human cytochrome P450 2B6 (2B6) has been proven to be a very important P450 for the metabolism of drugs and xenobiotics in liver, brain, kidney, and heart (*11, 12*). 2B6 metabolizes cyclophosphamide, efavirenz, bupropion, ifosfamide, and clopidogrel (*13*). Human P450 2E1 (2E1) is best known for its role in chemical activation/detoxication of chemical carcinogens and toxins, fatty acid metabolism, and the biotransformation of a large number of low molecular weight compounds and halogenated anesthetics such as enflurane and halothane (*14*). In addition to being found in the liver, 2E1 is also present in a number of other tissues including the brain and kidney. In the brains of alcoholics and alcoholic smokers, 2E1 is elevated in specific regions such as the pyramidal neurons of the cortex and hippocampus (*12*). 2B6 and 2E1 are also polymorphic enzymes with significant clinical and toxicological importance. 2E1 is known to have a smaller active site than other members of the P450 2 family. Therefore, it was of interest to compare the effects of PN on the structure and function of these two human P450s.

The addition of a nitro group to tyrosine lowers the pK_a of the hydroxyl group by 2–3 units, causing the normally hydrophobic tyrosine to be partially charged and to be more hydrophilic in the local environment. The additional bulky moiety may disrupt hydrogen bond networks or the structural integrity of protein, resulting in steric hindrance for the access of substrates or protein–protein interactions (*1, 15*). Thus a change in protein function may be expected as a result of the nitration of tyrosine. However, the selectivity with respect to the tyrosine to be nitrated is residue-, protein-, and tissue-specific (*5, 16*). By using LC-coupled electrospray ionization (ESI) in conjunction with tandem mass spectrometry (LC-MS/MS), a number of studies have reported specific sites for the nitration of tyrosine residues in tryptic peptides from PN-treated proteins (*15, 17–20*). This technique allows for the identification of the nitrated peptides on the basis of the mass shift of 45 Da (addition of NO_2 minus H). Based on a comparison of the MS/MS spectrum with the theoretical b and y ions, the specific site of nitrotyrosine formation in the peptide can be assigned. This is of particular value when more than one tyrosine is present in the tryptic peptide since the immunochemical methods that rely on the use of antityrosine antibodies cannot identify the exact residue(s) that has been modified by the addition of a nitro group (*21, 22*).

We have applied this same LC-MS/MS technique to investigate specific site(s) of tyrosine nitration in P450s 2B6 and 2E1 following the reaction with PN. After treatment of the P450s with various concentrations of PN, the NADPH-cytochrome P450 reductase (reductase)-supported and the *tert*-butylhydroperoxide (tBHP)-supported catalytic activities were compared. Modifications of the prosthetic heme were characterized by HPLC analysis, and the changes in the reduced-CO difference spectra were determined by UV–vis spectrophotometer. Homology modeling of 2B6 and 2E1 was performed in order to gain insight into the structural basis for the inactivation of these two P450s by PN.

Materials and Methods

Materials. PN was purchased from Cayman Chemicals (Ann Arbor, MI) and stored in 0.3 N NaOH at −80 °C prior to use. 7-Ethoxy-4-(trifluoromethyl)coumarin (EFC) was from Invitrogen Corp. (Carlsbad, CA). NADPH and tBHP were from Sigma-Aldrich Chemical Co. (St. Louis, MO). Sequencing-grade modified trypsin was from Promega (Madison, WI). All other chemicals and solvents used were of the highest purity available from commercial sources.

Purification of Enzymes. The expression vectors for human P450s 2B6 and 2E1 with their N-terminals truncated and their C-terminals His-tagged were expressed in *E. coli* TOPP3 cells, and the proteins were purified to homogeneity as previously described (*14*). Reductase was expressed and purified according to the methods described (*23*).

Enzymatic Activity Determinations. After treating the P450s (20 pmol in 80 μL of potassium phosphate buffer, pH 7.7) with various concentrations of PN (18.75, 37.5, 75, 150, 300, and 600 μM) for 5 min, the EFC *O*-deethylation activity was determined at 30 °C for 15 min in potassium phosphate buffer, pH 7.7, and compared to that of a control sample not exposed to PN as described previously (*21*). For the NADPH/reductase-supported activity, the samples were reconstituted with 40 pmol reductase for 30 min at 22 °C, and the activity remaining was determined using an assay mixture containing 100 μM EFC and 200 μM NADPH. For the tBHP-supported activity, the assay mixture contained EFC and tBHP at concentrations of 100 μM and 25 mM, respectively.

HPLC Analysis. An HPLC system (Waters 600E) was used to investigate the loss of native heme and the formation of heme adducts. Control and PN-treated samples (100 pmol of P450) were analyzed using a C4 reverse phase column (5 μm, 4.6 × 250 mm, 300 Å; Phenomenex, Torrance, CA). The solvent system consisted of solvent A (0.1% TFA/H_2O) and solvent B (0.05% TFA/acetonitrile). The column was eluted with a linear gradient from 30% to 80% B over 30 min at a flow rate of 1 mL/min, and the eluant was monitored at 400 nm. The absorption spectra of the native heme and the PN-modified heme adduct were determined using a Millipore model 996 diode-array detector.

Spectral Analysis. The reduced-CO difference spectra of the unmodified and PN-modified 2B6 and 2E1 were determined as described by Omura and Sato (*24*). Control and 600 μM PN-treated P450s (300 pmol of each) were reduced by the addition of reductase (600 pmol) and NADPH (0.5 mM) in the presence of substrate (500 μM benzphetamine for 2B6; 100 μM 4-methylpyrazole for 2E1) and then bubbled with CO. The UV–vis absorbance spectra were determined by scanning from 400 to 600 nm on a UV-2501 PC spectrophotometer (Shimadzu Corporation, Kyoto, Japan) until no further changes in the spectra were observed. A trace of sodium dithionite was added, and additional scans were performed until no further changes were observed.

Trypsin Digestion of 2B6 and 2E1. Control and PN-treated P450s (500 pmol of each) were denatured by incubation with 5 mM DTT at 60 °C for 45 min and then exhaustively dialyzed against 100 mM ammonium bicarbonate at pH 8.0. The samples were digested with trypsin at 37 °C for 24 h and then subjected to LC-ESI mass spectrometry on a LCQ mass analyzer (Thermo Electron Corporation, Waltham, MA) to identify unmodified and modified peptides. The specific site of nitration was determined by MS/MS fragmentation on the LCQ. The predicted enzymatic full mass spectrum and fragmentation to give the b and y ions of the tryptic peptides was obtained using the ProteinProspector (http://prospector.ucsf.edu/) computer program.

LC/MS/MS Analysis of Tryptic Peptides. Samples were analyzed on a C18 reverse phase column (Luna, 3 μm, 4.6 × 100 mm, Phenomenex, Torrance, CA) using isocratic elution with 20% B for 5 min followed by a linear gradient to 70% B over 30 min and to 90% B over 10 min at a flow rate of 0.2 mL/min. The solvent system consisted of solvent A (0.1% formic acid/H_2O) and solvent B (0.1% formic acid/acetonitrile). The column effluent was directed into an LCQ mass analyzer (Thermo Electron Corporation). The ESI conditions were sheath gas, 90 arbitrary units; auxiliary gas,

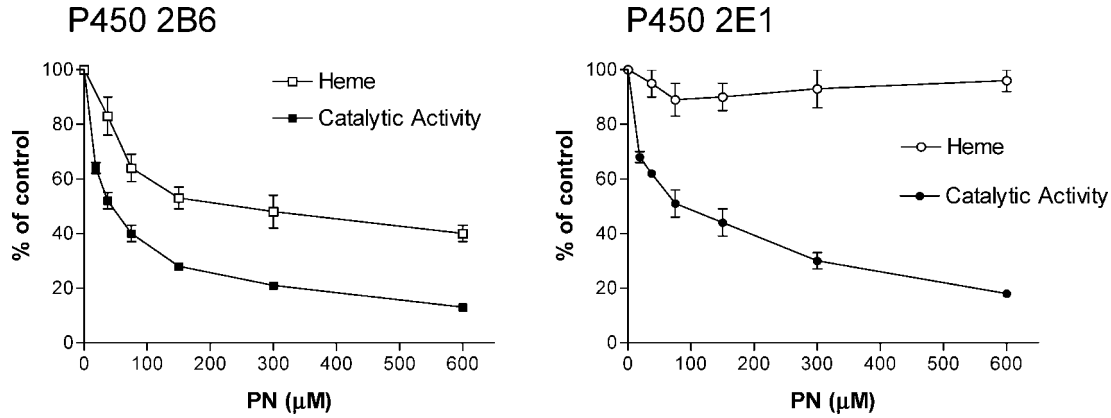

Figure 1. Effect of PN on NADPH/reductase-supported catalytic activity and native heme remaining from P450s. P450s 2B6 and 2E1 were treated with 18.75, 37, 75, 150, 300, and 600 μM PN as indicated, and the residual EFC catalytic activity supported by NADPH/reductase was determined. Native heme remaining after treatment with the various concentrations of PN was determined by HPLC. The experimental conditions and analyses are described in Materials and Methods. The % of control denotes the relative catalytic activities and relative amounts of native heme remaining as assessed by comparison to untreated P450s. Each point shown represents the mean from three separate experiments done in duplicate. The control (100%) catalytic activities for 2B6 and 2E1 are 330 ± 21 and 125 ± 10 pmol of 7-hydroxy-4-trifluoromethylcoumarin produced/min/nmol P450, respectively.

30 arbitrary units; spray voltage, 3.5 kV; capillary temperature, 200 °C; capillary voltage, 45 V; and tube lens offset, 25 V. Data were acquired in positive mode using the Excalibur software package (Thermo Electron Corporation) with one full scan followed by two data-dependent scans of the second most intense and the third most intense ion.

LC-ESI-MS Analysis of the Heme Adduct. To characterize the mass of the heme adduct, samples containing 1 nmol of control and PN-treated 2B6 in 1 mL of 100 mM potassium phosphate buffer, pH 7.7, were extracted with 1 mL of 2% TFA/acetonitrile, and the extracts were concentrated using Amicon Ultra Centrifugal Filter Devices (Millipore Corporation, Billerica, MA). The samples were analyzed on a C4 reverse phase column (5 μm, 2 × 150 mm, Phenomenex, Torrance, CA) using a linear gradient from 35% to 65% B over 20 min and then to 95% B over an additional 10 min with a flow rate of 0.3 mL/min. The solvent system was the same as that in the HPLC analysis of heme modification as described above. The ESI conditions were sheath gas, 90 arbitrary units; auxiliary gas, 30 arbitrary units; capillary temperature, 180 °C; and spray voltage, 3.5 kV. Data were acquired in positive ion mode using Excalibur software (Thermo Electron) with one full scan followed by two data-dependent scans of the most intense and the second most intense ion.

Homology Modeling. Homology modeling was performed using SPDB-Viewer (*25, 26*). In the absence of crystal structures for 2B6 and 2E1, the crystal structure of cytochrome P450 2B4 complexed with 4-chlorophenylimidazole (PDB code 1SUO) (*27*) was used as the template for homology modeling. The accuracy of a modeled structure depends on the extent of homology between the proteins. 2E1 has 75% sequence identity with 2B4, and 2B6 has 85% sequence identity with 2B4. Briefly, the sequences of 2B6 and 2E1 were aligned with the sequence of 2B4 using ClustalW[ii] and validated in the SPDB-Viewer. A crystal structure of the $P450_{BM3}$ heme binding domain and the FMN binding domain was taken as the basis for modeling the complexes of 2E1 or 2B6 with reductase (*28*). The 2E1 or 2B6 homology model was superimposed with the heme domain of the $P450_{BM3}$ complex, and the FMN domain of human reductase was superimposed with the FMN domain of $P450_{BM3}$. The amino acids involved in protein–protein interactions from the obtained complexes were analyzed. The modeling request was submitted to the SWISS-MODEL comparative protein modeling server. The stereochemistry of the obtained models was evaluated to ensure the correct structure. The graphics were done with the DS Viewer (Accelrys, CA).

Results

NADPH/Reductase-Supported Catalytic Activity. Following the exposure of 2B6 and 2E1 to various concentrations of PN, the NADPH/reductase-supported catalytic activity remaining was determined with the activity of untreated P450 as the 100% control. As shown in Figure 1, exposure to PN decreases the enzymatic activity of both 2B6 and 2E1 in concentration-dependent manner with the concentration giving 50% inhibition at ~40 μM and ~75 μM, respectively.

Heme Modification. The effect of PN on 2B6 and 2E1 was investigated by HPLC under acidic conditions to monitor changes in the amounts of native heme (Figure 1 and Figure 2A). For 2B6, the native heme was modified in a dose-dependent manner, but the amount of heme modification observed was less than the decrease in the enzymatic activity, as shown in Figure 1. For 2E1, there was no significant loss of native heme even after incubation with 600 μM PN when loss of catalytic activity exceeded 80%. These results suggest that modification of the P450 heme by PN can only partially account for the inactivation of 2B6 and that the rest of the inactivation is due to modification of protein. The major contribution to the loss of 2E1 enzymatic activity supported by NADPH/reductase is due to protein modification.

Formation of the Heme Adduct in 2B6. Figure 2A shows representative HPLC traces that demonstrate the loss of heme as a result of exposure to increasing concentrations of PN. In addition to heme loss, at higher concentrations of PN, a heme adduct that eluted later than the native heme (Figure 2B) was observed. The maximal absorbances in the UV spectrum for the native heme and the heme adduct occur at 398 nm and 407 nm, respectively (Figure 2C). The maximum for the Soret peak at 407 nm for the heme adduct indicates that the heme is modified. LC-MS/MS analysis revealed that a heme-derived ion with the MH^+ ion at m/z 661 was observed in the PN-treated sample but not in the control sample (Figure 2D and inset). The mass increase of 45 Da compared to the native heme with the ion at m/z 616, suggested that a nitro group had been inserted into one of the pyrrolic rings. Similar modifications forming nitrated heme have been reported in studies of the reaction of human myoglobin with nitrite and hydrogen peroxide (*29*). Proton NMR analysis of the nitrated heme from hemoglobin demonstrated that the site of modification is a vinyl group that

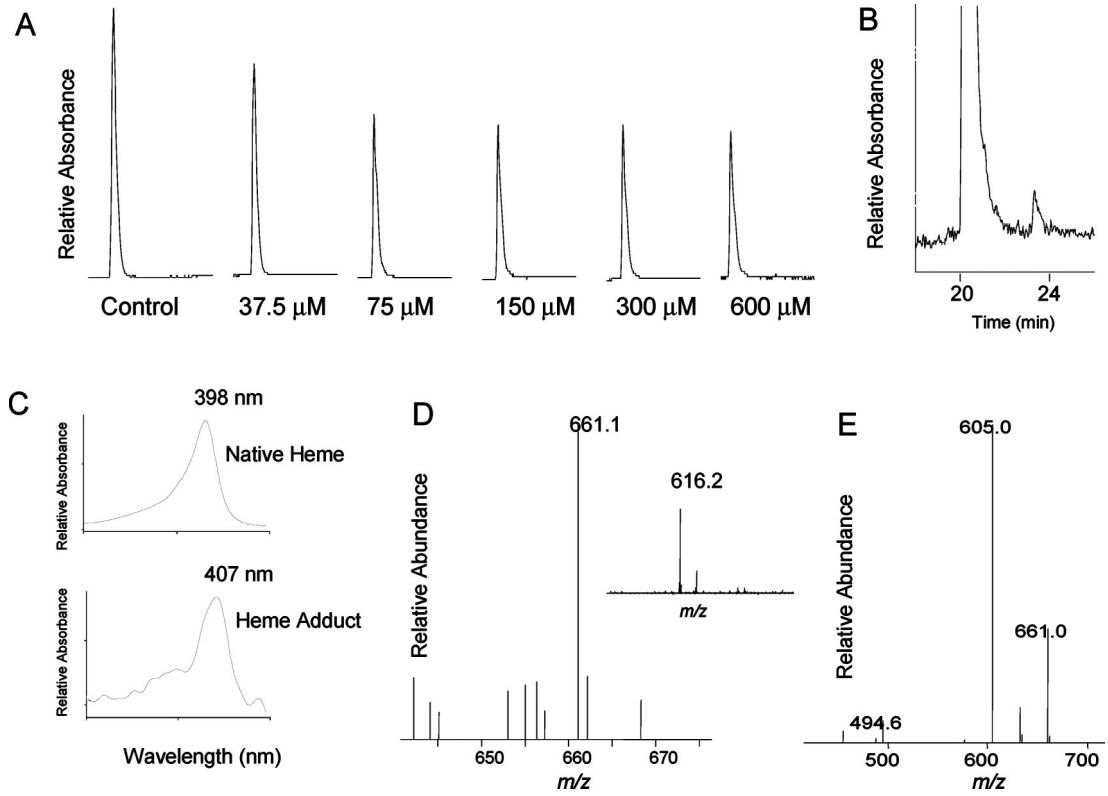

Figure 2. Modification of the 2B6 heme after incubation with various concentrations of PN. The untreated and PN-treated (37.5, 75, 150, 300, and 600 μM PN) P450 2B6 samples were analyzed by HPLC under acidic conditions as described in Materials and Methods. A shows representative HPLC chromatograms of the native heme remaining monitored at 398 nm following exposure to the concentrations of PN indicated. All of the heme peaks eluted at ~21.5 min. B is an enlarged scale of the HPLC chromatogram from the sample treated with 600 μM PN showing that the native heme and the heme adduct eluted at 21.5 min and 23.5 min, respectively. C shows that the maximal absorption of the Soret peaks for the native heme and the heme adduct determined with a diode-array detector are at 398 nm and 407 nm, respectively. D shows the full mass spectrum of the nitroheme with *m/z* 661 in LC-MS analysis. The inset shows the data from a control. E shows the MS/MS spectrum of the nitroheme with *m/z* 661.

is converted to a nitrovinyl group by substitution of a proton by the NO_2 group (*30*). The MS/MS spectrum of the nitroheme adduct is displayed in Figure 2E. The fragment ion at *m/z* 605 is probably due to the loss of iron.

Nitration of Tyrosine Residues in 2B6. Nitration of tyrosine was detected by LC-MS/MS analysis by the characteristic shift in the mass of 45 Da because of the addition of the nitro group. After exposure of 2B6 to 150–600 μM PN followed by tryptic digestion, LC-MS/MS analysis revealed that tyrosine residues in four tryptic peptides were nitrated: Tyr244 in the tryptic peptide-spanning residues 237–251 (NLQEINAYIGHSVEK), Tyr268 in the sequence spanning 263–274 (DLIDTYLIHMEK), Tyr354 in the sequence spanning 346–358 (MPYTEAVIYEIQR), and Tyr380 in the sequence 379–384 (GYIIPK). All of the major MS/MS fragmentation peaks for the four unmodified peptides matched their theoretically predicted patterns as determined using ProteinProspector software (data not shown).

1. Nitration of Tyr354. The theoretical b and y ion fragments for the tryptic peptide sequence 346–358 are displayed in Figure 3A. The extracted ion chromatogram shows that the unmodified peptide (*m/z* 1612.7) eluted at 18.6 min and the nitrated peptide (*m/z* 1657.7) eluted at 19.8 min (Figure 3B). A representative MS/MS spectrum for the singly charged precursor ions is displayed in Figure 3C. The presence of b product ions from b5–b8 matches that for the theoretical unmodified fragment ions and product ions with an increase of 45 Da are observed for ions b9–b11 and y5–y12, indicating that the second tyrosine residue in this tryptic peptide, corresponding to position 354, is nitrated. Small fragment ions corresponding to unmodified b3, b4, y2, y3, and the predominant fragmentation peak at *m/z* 753 corresponding to y5 + 45 were observed in the MS/MS spectrum of the doubly charged tryptic peptide (data not shown). Thus, Tyr354 is the target for modification by PN yielding nitrotyrosine in this tryptic peptide. LC-MS/MS analysis allows for the identification of the specific residue that was modified when there were multiple tyrosine residues in a single peptide from a tryptic digest. Masses corresponding to the nitration of two tyrosine residues were not detectable.

2. Nitration of Tyr244, Tyr268, and Tyr380. The identification of nitration at residues 244, 268, and 380 is shown in Figures S1, S2, and S3, respectively (Supporting Information).

Nitration of Tyrosine Residues in 2E1. After the treatment of 2E1 with 150–600 μM PN followed by trypsin digestion, LC-MS/MS analysis revealed that four tyrosine residues were nitrated: Tyr69 in the peptide sequence spanning residues 62–74 (FGPYFTLYVGSQR), Tyr317 in the peptide sequence spanning residues 317–323 (YPEIEE), Tyr380 in the sequence spanning residues 379–384 (GYLIPK), and Tyr422 in the sequence spanning residues 422–433 (YSDYFKPFSTGK). The MS/MS spectra of the major product ions from all four unmodified peptides match the predicted b ions and y ions obtained from the ProteinProspector software (data not shown).

1. Nitration of Tyr422 and Tyr380. The predicted b and y ion fragments for the unmodified peptide spanning residues 422–433 are displayed in Figure 4A. The extracted ion chromatogram shows that the unmodified peptide (*m/z* 1439.4) elutes at 14.3 min and that the nitrated peptide (*m/z* 1484.4) elutes at 16.6 min (Figure 4B). The MS/MS fragmentation pattern of the doubly charged peptide shown in Figure 4C reveals the

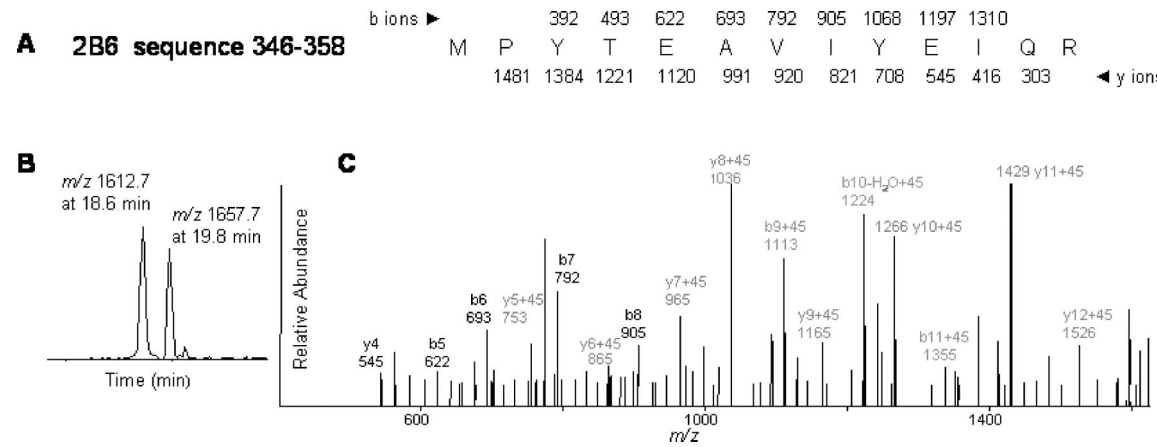

Figure 3. LC-MS/MS analysis of nitrated residue at position 354 of 2B6. P450 2B6 was treated with 300 μM PN, digested with trypsin and then subjected to LC-MS/MS analysis as described in Materials and Methods. (A) Sequence of the unmodified tryptic peptide spanning residues 346–358 with the predicted b and y series ions indicated. (B) Extracted ion chromatograms of the unmodified peptide 346–358 (*m/z* 1612.7) eluting at 18.6 min and its nitrated peptide (*m/z* 1657.7) eluting at 19.8 min. (C) MS/MS spectrum of the nitrated peptide with *m/z* 1657.7. The MS/MS spectra were obtained in positive mode using the Excalibur software package, and the identification of modified nitrotyrosine residues at Y354 is discussed in the text.

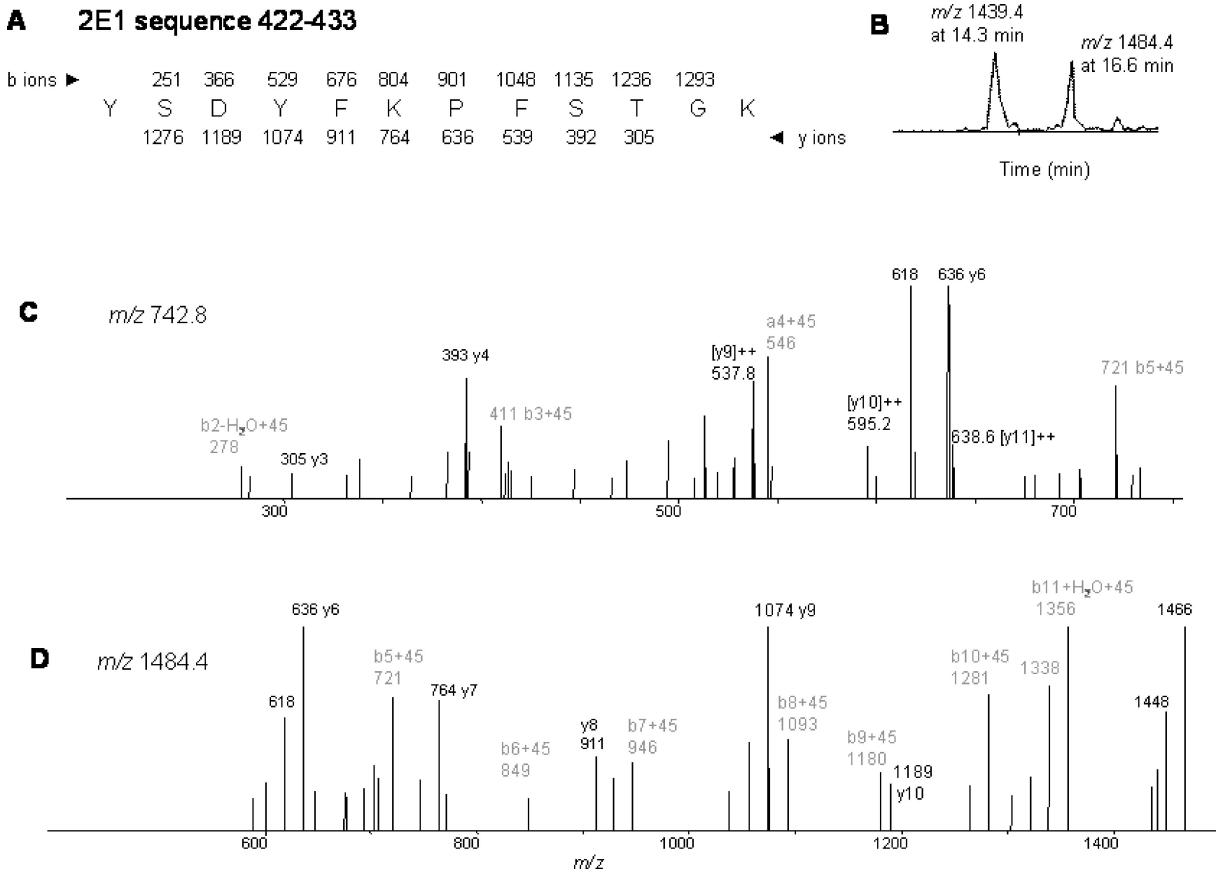

Figure 4. LC-MS/MS analysis of the nitrated residue at position 422 of P450 2E1. (A) Sequence of the unmodified peptide 422–433 with the predicted b and y series ions indicated. (B) Extracted ion chromatograms of the unmodified peptide (*m/z* 1439.4) eluting at 14.3 min and the nitrated peptide (*m/z* 1484.4) eluting at 16.6 min. (C) MS/MS spectrum of the doubly charged nitrated peptide with *m/z* 742.8. (D) MS/MS spectra of the singly charged nitrated peptide with *m/z* 1484.4. The spectra were obtained in positive mode using the Excalibur software package, and the identification of the modified nitrotyrosine residue at Tyr422 is discussed in the text.

addition of one nitro group to the b2–b5 ions, and the singly charged MS/MS fragmentation pattern shown in Figure 4D reveals the addition of one nitro group to the b5–b11 ions. Although there are two tyrosine residues in this tryptic peptide, on the basis of the absence of the additional nitro group on the y9, y10, and y11 ions as shown in Figure 4C and D, the nitrated tyrosine residue is assigned to be the Tyr422 residue. This provides another example of where it is possible to identify the specific site of tyrosine nitration by LC-MS/MS analysis in peptides where two or more tyrosine residues exist in the same tryptic peptide. The sequence for the Tyr380 containing tryptic peptide and the MS/MS spectra in 2E1 is similar to that in 2B6, thus the MS/MS spectra are not shown and the conclusion is that Tyr380 was nitrated.

Table 1. Summary of All of the Nitrotyrosine Containing Peptides Identified in PN-Treated P450s 2B6 and 2E1 after Trypsin Digestion

P450[a]	position of nitrated Tyr[b]	sequence	*m/z* of the unmodified peptide	*m/z* of the NO_2-modified peptide
2B6	244	^{237}NLQEINA-Y-IGHSVEK^{251}	1714.6	1759.6
	268	^{263}DLIDTU-Y-LIHMEK^{274}	1490.5	1535.5
	354	^{346}MPYTEAVI-Y-EIQR^{358}	1612.7	1657.7
	380	^{379}G-Y-IIPK^{384}	690.3	735.3
2E1	69	^{62}FGPVFTL-Y-VGSQR^{74}	1470.6	1515.6
	317	^{317}Y-PEIEEK^{323}	907.3	952.2
	380	^{379}G-Y-LIPK^{384}	690.3	735.3
	422	^{422}Y-SDYFKPFSTGK^{433}	1439.4	1484.4

[a] P450 was treated with PN, dialyzed against 100 mM ammonium bicarbonate, pH 8.0, digested with trypsin, and the peptides subjected to LC-MS/MS analysis as described in Materials and Methods. [b] The identification of the sites of nitration was illustrated in Figures 3–4 and Figures S1–S5 (Supporting Information).

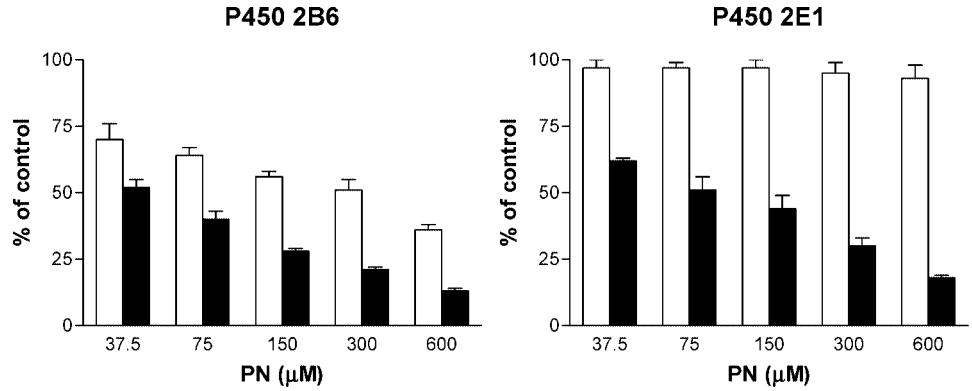

Figure 5. Comparisons of the tBHP- (□) and NADPH/reductase- (■) supported catalytic activities of P450s 2B6 and 2E1 after reaction with PN. P450s 2B6 and 2E1 were treated with PN at the concentrations indicated, and the EFC *O*-deethylation activity remaining was determined as described in Materials and Methods. The data presented are from three separate experiments done in duplicate. The control (100%) catalytic activities for 2B6 supported by NADPH/reductase and tBHP are 330 ± 21 and 109 ± 10 pmol of 7-hydroxy-4-trifluoromethylcoumarin produced/min/nmol P450, respectively. The control (100%) catalytic activities for 2E1 supported by NADPH/reductase and tBHP are 125 ± 10 and 31 ± 5 pmol of 7-hydroxy-4-trifluoromethylcoumarin produced/min/nmol P450, respectively.

2. Nitration of Tyr69 and Tyr317. The identification of nitration at residues 69 and 317 is shown in Figures S4 and S5, respectively (Supporting Information).

Extent of Nitrotyrosine Formation. After the treatment of P450s 2B6 and 2E1 with PN ranging from 18.75 μM to 600 μM, the extent of nitrotyrosine formation in the individual tryptic peptide fragments was determined by integration of the peak areas of the individual nitrated peptides relative to the total peak area of the native and nitrated peptides in the extracted ion chromatograms. The results showed that the extent of nitration for the individual nitrotyrosine-containing peptides correlated well with increasing concentrations of PN used for the inactivation. For instance, the extent of the nitro-Tyr354-containing peptide detected in 2B6 was 8, 12, 23, 41, and 56% following PN exposure to 37.5, 75, 150, 300, and 600 μM PN, respectively. At low concentrations of PN, the most prominently nitrated residue in 2B6 was Tyr354 followed by Tyr268 and Tyr244. Under the same conditions, primarily Tyr422 and Tyr317 were nitrated in 2E1, and Tyr69 was modified to a lesser extent. In both 2B6 and 2E1, nitration of Tyr380 was relatively minor and was not observed at PN concentrations less than 75 μM.

In conclusion, four tyrosine residues in 2B6 and four in 2E1 were identified as being nitrated by ESI-LC-MS/MS analysis. The extracted ion chromatograms reveal that all of the nitrotyrosine-containing peptides have slightly longer retention times than their corresponding unmodified peptides. The fact that the nitro group of the nitrotyrosine in the nitrated peptide is stable to electrospray ionization mass spectrometry allowed for the almost complete assignment of the observable b and y fragment ions exhibiting the expected increase of 45 Da. In contrast, MALDI-MS of nitrated peptides leads to extensive fragmentation due to the cleavage of the nitro group with the elimination of one or two oxygens. Therefore, the resulting ions may obscure the assignment of specific nitration sites (*31–33*). The positions of the nitrated tyrosine residues, the amino acid sequences of the tryptic peptides, and the masses of unmodified and NO_2-modified peptides for PN-treated 2B6 and 2E1 are summarized and shown in Table 1.

tBHP-Supported Catalytic Activity of the Modified Proteins. In order to investigate whether inactivation of the protein modified by PN is due to the interference with substrate binding, the interaction of the P450 with reductase, or another step in the overall reaction, the EFC catalytic activity supported by tBHP was characterized and compared to that supported by NADPH/reductase. As shown in Figure 5, both 2B6 and 2E1 exhibit concentration-dependent losses in EFC catalytic activity, when the reactions are supported by NADPH/reductase. For 2B6, although a loss in the EFC activity supported by tBHP is observed and is dependent on the PN concentration, the extent of activity loss is less than that when the reaction is supported by NADPH/reductase. Interestingly, there is no significant loss in the tBHP-supported EFC catalytic activity with 2E1, even when the loss of NADPH/reductase-supported activity is greater than 80%. For both P450s, the catalytic activity remaining supported by tBHP correlates very well with the native heme remaining as shown in Figure 1, suggesting that protein modification by PN does not interfere with substrate binding and its metabolism, at least in the case of EFC. Since hydroperoxides and other artificial oxygen donors are able to support the catalytic turnover of P450 in the absence of electron transfer proteins such as the reductase (*34, 35*), the much more

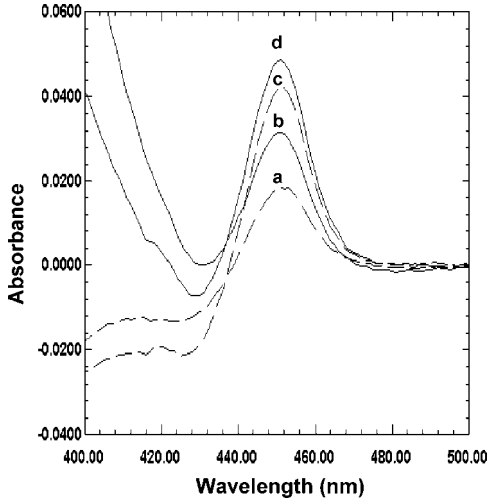

Figure 6. Effect of PN on the ability of P450 2E1 to exhibit a reduced-CO difference spectrum. The reduced-CO difference spectra of untreated (c) and PN-treated (a) P450 were determined after the samples were reduced by NADPH/reductase and then bubbled with CO as described in Materials and Methods. Spectrum d was obtained following the addition of a trace of dithionite to c. Spectrum b was obtained following the addition of a trace of dithionite to a. The wavelength for maximal absorbance is at 451 nm for both the untreated and PN-treated P450s.

extensive effect on activity loss supported by NADPH/reductase as compared to that supported by tBHP suggests that the inactivation due to protein modification by PN might occur as a result of the interaction impairing the binding of the P450s with reductase, interference with electron transfer pathways, or other steps in the catalytic cycle.

Reduced-CO Difference Spectra. As shown in Figure 6, the reduced-CO difference spectrum of 2E1 that was exposed to 600 μM PN and then reduced enzymatically with NADPH/reductase is ~46% of that of 2E1 not exposed to PN (a versus c). Because there was no significant loss of heme in 2E1 (Figure 1), these results suggest that the modified protein has lost some of its ability to accept electrons from NADPH/reductase and to bind the CO. Following the addition of dithionite, the level of the ferrous-carbonyl complex increased ~15% for untreated 2E1 (d versus c) and increased 65% for PN-treated 2E1 (b versus a). Thus, it appears that the transfer of the first electron from NADPH via reductase to the heme iron in PN-modified 2E1 is partially impaired. Moreover, the relative level of dithionite-reduced CO spectra for PN-modified 2E1 is ~61% of untreated 2E1 (b versus d) and no detectable P420 is observed. These results suggest that the heme-thiolate ligation is not destroyed by PN, but the coordination of heme with the other axial ligand in the protein may be partially altered by PN. Under the same experimental conditions, similar phenomena were observed for the levels of the reduced-CO spectra remaining in PN-treated 2B6. For the 600 μM PN-treated 2B6, the formation of reduced-CO complex either enzymatically with NADPH/reductase (15% of control) or chemically with dithionite (25% of control) is much less than the native heme content remaining (43% of control).

Homology Modeling of 2B6 and 2E1 and their Complexes with Reductase. The homology models of 2B6 and 2E1 were constructed using 4-chlorophenylimidazole-bound 2B4 as the template (*25–27*). The model structures of 2B6 and 2E1 are shown in Figures 7 and 8, and the locations of the four nitrated residues are illustrated. The residues within 5 Å of the nitrated tyrosine residues are displayed separately in Figures 7 and 8 for 2B6 and 2E1, respectively. Tyr 69 of 2E1 and Tyr380 of 2B6/2E1 are surface residues and are completely exposed to the solvent. In addition, they are surrounded by Pro and Arg. Tyr244/Tyr268/Tyr354 of 2B6 and Tyr317/Tyr422 of 2E1 are all partially exposed to solvent. The common features for these residues are that they are surrounded by Glu/Asp and Phe in a relatively hydrophobic environment. Models of the 2B6–reductase complex and the 2E1–reductase complex were built to determine whether the nitrated residues were located in or near the P450 binding site for the reductase. The P450–reductase complexes were generated by superimposing the heme of the models of 2B6 and 2E1, and the FMN domain of cytochrome P450 reductase on the crystal structure of the complex between cytochrome $P450_{BM3}$ and the FMN domain of the $P450_{BM3}$ reductase (*28*). The relationships between Tyr354 and Arg443 of 2B6 and the FMN domain of the reductase and the relationship between Tyr422 of 2E1 and the FMN domain of the reductase are shown in Figure 9A and 9B, respectively. Tyr354 of 2B6 forms a hydrogen bond with Arg 443, which has been implicated by site-directed mutagenesis in binding reductase (*36*), while Tyr422 of 2E1 is also likely to be at the reductase binding site. Tyr422 of 2E1 corresponds to Arg422 of 2B4. Arg422 has been shown to be involved in binding reductase (*36*). Hence, the two most readily modified tyrosines in 2B6 (Tyr354) and 2E1 (Tyr422) are located in/near the reductase binding site on cytochrome P450. Tyrosine 422 is within 5 Å of the FMN cofactor in the model complex.

Discussion

The effects of PN on two human P450s, 2B6 and 2E1, were characterized. After exposure to PN, heme modification of 2B6 was observed, but there was no modification of the heme in 2E1. For 2B6, the catalytic activity remaining supported by tBHP correlated with the amount of heme remaining, and they both decreased in a concentration-dependent manner. The activity remaining supported by tBHP was greater than that supported by NADPH/reductase. For 2E1, the catalytic activity supported by tBHP and the amount of heme remaining did not decrease significantly even at high concentrations of PN, but the catalytic activity supported by NADPH/reductase was dramatically decreased. The P450 catalytic cycle consists of a number of discrete steps that could be affected by protein modification, leading to a loss of activity (*34, 35*). These include substrate binding, transfer of the first electron, oxygen binding, transfer of the second electron, activation of the oxygen, insertion of activated oxygen into substrate, and product release. Alkyl hydroperoxides such as tBHP can serve as alternate oxygen sources to support the reaction in place of NADPH/reductase. The differences in the extent of inactivation observed in 2B6 and 2E1 when the reactions are supported by tBHP and NADPH/reductase suggest that PN-mediated protein modification does not interfere with substrate binding, oxygen insertion, or product release. However, the decrease in the levels of the reduced-CO complex when the reduction is supported by NADPH/reductase and further increases observed following the addition of dithionite suggest that the pathways for electron transfer from FMN in the reductase to the P450 heme were partially impaired in both the modified 2B6 and 2E1 and that they may contribute to activity loss.

Four tyrosine residues of the 15 tyrosine residues in 2B6 and 2E1 were shown to be nitrated. Previous studies have shown that protein nitration appears to be a selective process and that several factors play a role in directing nitration to specific tyrosine residues. These factors include protein folding, the presence of a transition metal, exposure of the residue on the

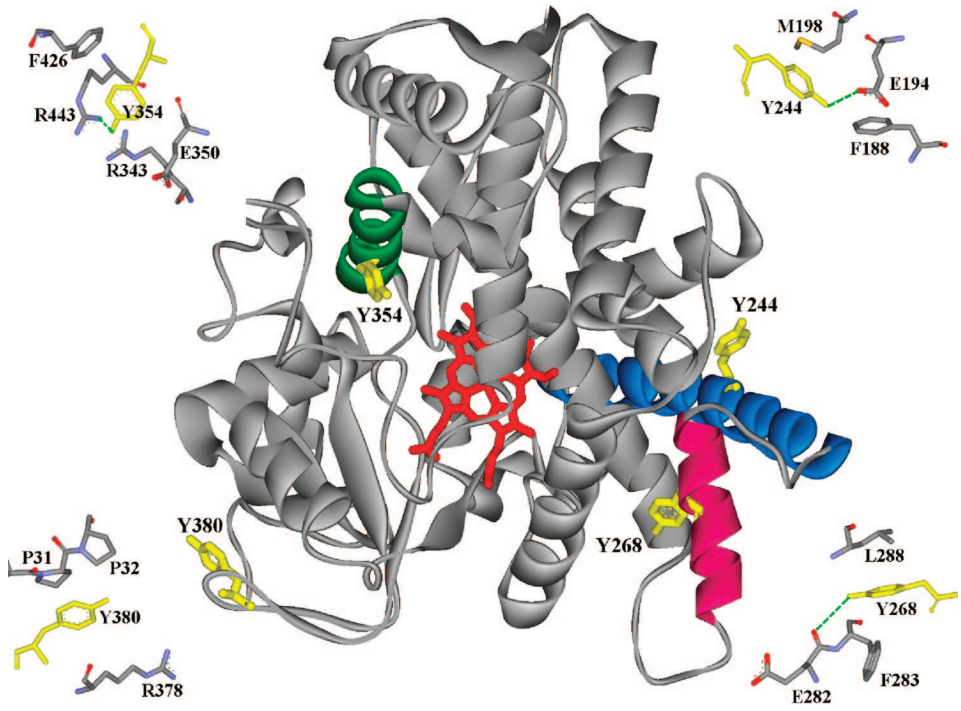

Figure 7. Homology model of P450 2B6 showing the four nitrated tyrosine residues. This structure was constructed on the basis of the crystal structure of P450 2B4 as described in Materials and Methods. Shown in color are the heme (red), the tyrosine residues (yellow), the G helix (blue), the H helix (magenta), and the K helix (green). Each of the nitrated tyrosine residues (244, 268, 354, and 380) and the residues within 5 Å of them are shown separately for clarity. Potential hydrogen-bonding interactions between the tyrosine residues and neighboring residues are indicated by using the green dashed lines. The distances from the heme iron to Y354, Y268, Y244, and Y380 are 15, 18, 21, and 30 Å, respectively.

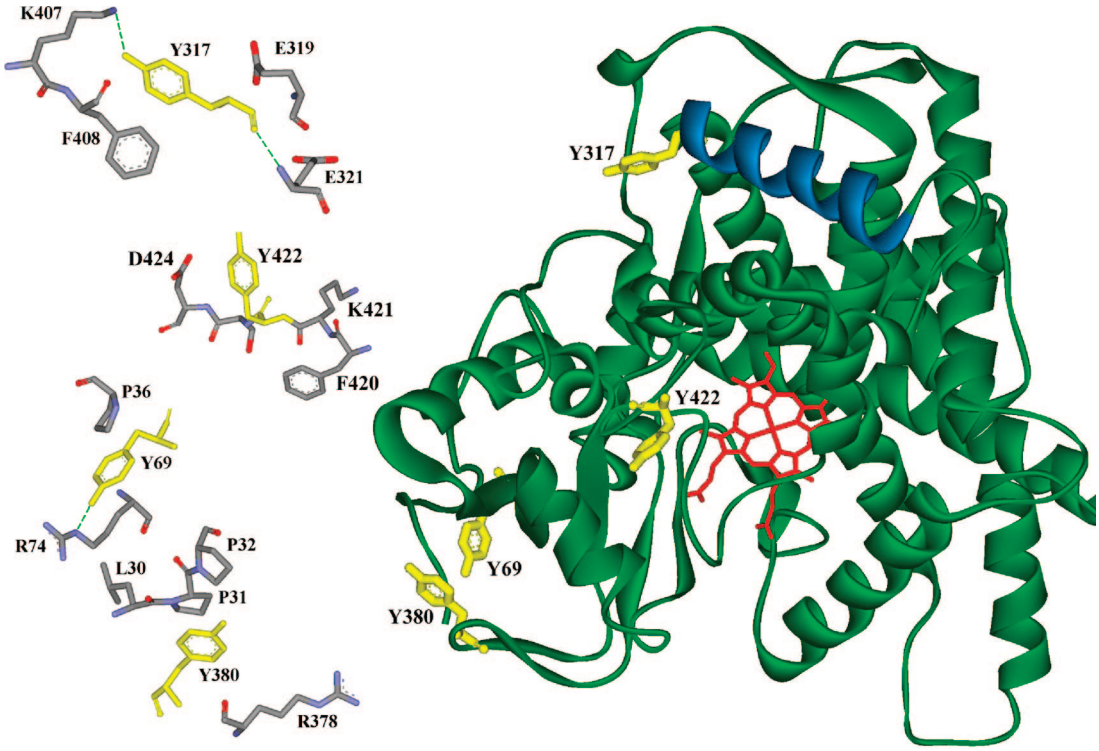

Figure 8. Homology modeling of P450 2E1 showing the four nitrated tyrosine residues. This structure was constructed based on the crystal structure of P450 2B4 as described in Materials and Methods. Shown in color are the heme (red), the tyrosine residues (yellow), and the J helix (blue). Each of the nitrated tyrosine residues (69, 317, 380, and 422) and the residues within 5 Å of them are shown separately for clarity. Potential hydrogen bonding interactions between the tyrosine residues and neighboring residues are indicated by the green dashed lines. The distances from the heme iron to Y422, Y317 and Y69/Y380 are 17, 20, and 30 Å, respectively.

surface of protein, neighboring negatively charged residues, and the secondary structure of protein (*2, 16, 18, 37*). In this study, homology modeling has shown some common features of the residues within 5 Å of the target tyrosine residues (Figures 7 and 8): (a) residue 380 of 2B6 and residues Tyr69/ Tyr380 of 2E1 are on the surface and are in close proximity to a Pro and an Arg, and (b) all of the other target residues have either Glu or Asp and Phe in close proximity. Interestingly, residues Tyr69 and Tyr380 of 2E1 are adjacent to each other in the homology model, but Tyr69 is more readily nitrated. Moreover, tyrosine

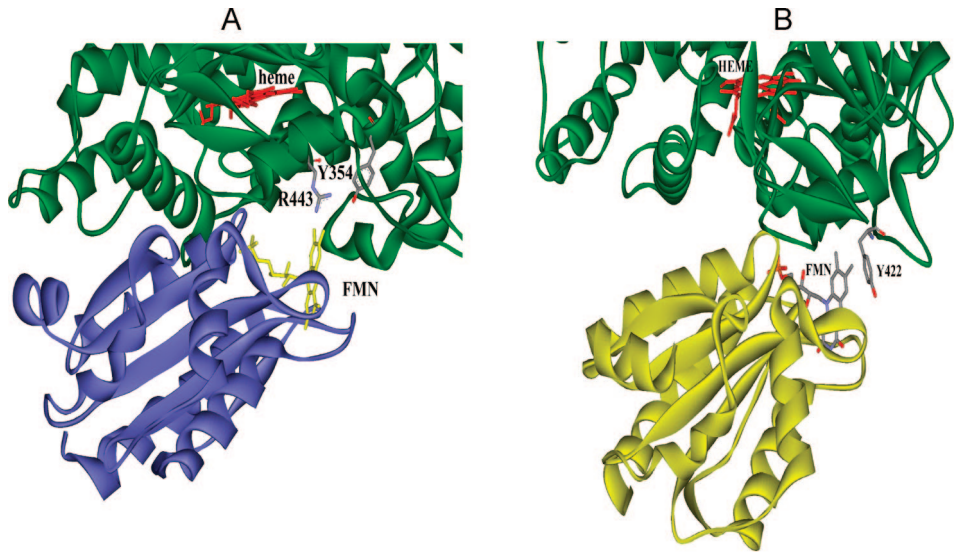

Figure 9. Homology models of the proximal sides of the P450s and their complexes with the FMN domain of reductase. The structures show a potential interaction of Tyr354 in 2B6 and Tyr422 in 2E1 with reductase on the basis of the $P450_{BM3}$ crystal structure. (A) 2B6–reductase complex. Shown in color are the P450 (green), the reductase (blue), the heme (red), and the relationship of Tyr354, R433, and the FMN cofactor. (B) 2E1–reductase complex. Shown in color are the P450 (green), the reductase (yellow), the heme (red), and the relationship of Y422 and the FMN cofactor. Tyr422 is approximately 5 Å away from the FMN cofactor.

244 in 2E1 and tyrosine 317 in 2B6 are not susceptible to nitration. Our homology modeling results also indicate that residues other than Glu/Asp may be in close proximity to the tyrosine (homology model not shown). For example, in 2E1, residue 194 is Lys instead of Glu, and in 2B6, residue 319 is His instead of Glu, and residue 321 is Ala instead of Glu (Figures 7 and 8). Taken together, our results support the hypothesis that local hydrophobic secondary structure surrounding the tyrosine residue with Glu/Asp in close proximity may be an important factor in directing nitration and that the location/primary structure may not be so important. Nitration of a tyrosine in proteins that is facilitated by the presence of a neighboring Glu/Asp has been shown in the following cases: Tyr17 in the rod and head domains of neurofilament-L (*15*), Tyr45 and Tyr193 in human mitochondrial superoxide dismutase (*18*), Tyr190 in P450 2B1 (*21*), Tyr99 in calmodulin (*37*), and Tyr108 in bovine Cu,Zn superoxide dismutase (*38*). In summary, the site of nitrotyrosine formation in proteins appears to be selective, but the precise role of the negative charge on Glu or Asp in directing the nitration of a neighboring tyrosine residue is not yet well understood (*15, 16*).

Previous studies from several laboratories have reported that nitration of one or two specific tyrosine residues in a protein may be sufficient to disrupt the protein structure, affect catalytic activity, or impair the regulatory function of the protein in complex biological systems (*15, 17, 21, 35, 37, 39–42*). Addition of a nitro group to a tyrosine lowers the pK_a of its phenolic hydroxyl group by 2–3 units and adds a bulky moiety. The potential consequence of such nitration may cause a normally hydrophobic tyrosine to become partially charged and thus be more hydrophilic, thereby altering electrostatic interactions. It may also disrupt the hydrogen bonding critical for the structural integrity of P450; hence, the amino acid pathway within the protein responsible for electron transfer may be modified (*1, 6, 15*). The reductase-dependent catalytic activity of P450 requires an optimized orientation of the P450-reductase on the P450 for electron transfer. PN-mediated P450 nitration may have an effect on (1) the conformational and electrostatic interactions between P450 and reductase and (2) any step in the P450 catalytic cycle. Although LC-MS/MS analysis has shown that a total of four tyrosine residues are nitrated in 2B6 and 2E1 in the presence of high concentrations of PN, in 2B6, at low PN concentrations where there was 40% loss in activity, only Tyr354 was modified and therefore is probably the major contributor for the inactivation. In 2E1, under the same conditions, two tyrosine residues were modified; thus, either Tyr422 or Tyr317 will be the major contributor. On the basis of the results of the site-directed mutagenesis and homology modeling, Arg443 and Arg422, which are on the proximal surface of P450 2B4, have been shown to be involved in reductase binding (*36, 43*). Modeling based on the $P450_{BM3}$ reductase complex suggests that Tyr422 in 2E1 is in close proximity to FMN in the reductase. The formation of nitrotyrosine, a negatively charged and hydrophilic moiety, is expected to change the function of the protein. Thus, the pathway for electron transfer from NADPH via reductase to the heme iron involving amino acid residues in P450 might be expected to be altered by the addition of a nitro group to Tyr422. The results of our homology modeling shown in Figure 9 indicate that there is hydrogen bonding between Tyr354 and Arg443 of 2B6. In addition, Phe426 is within 5 Å of Tyr354, and it is adjacent to the methylene bridge of the porphyrin ring. Homology modeling of 2B6 complexed with the reductase shows that Arg443 also interacts with the FMN domain of reductase. It is highly likely that the addition of a nitro group to Tyr354 may disrupt the hydrogen bonding and that this modification of 2B6 can interfere with the electron transfer through Arg443-Phe426 to the heme center. Therefore, it is no longer catalytically competent when compared to the untreated 2B6. Although the nitration of Tyr380 was not observed at low concentrations of PN, its contribution to inactivation at high PN concentrations cannot be ruled out. Previous studies have led to the suggestion that Tyr380 and Lys384 of P4502B4 and Tyr243 and Tyr271 of P450 1A2 are functionally involved in the interactions of NADPH-cytochrome P450 reductase with these two P450s (*44, 45*). It has also been reported that hydrogen bonding between Tyr64 and Lys63 in cytochrome c_{553} is essential for electron exchange with formate dehydrogenase (*46*). It appears that the aromatic ring of tyrosine and the basic charge of the Lys/Arg residue may contribute to the stabilization of the hydrophobic core for electron transfer. Lys residues are next to Tyr317 and Tyr422 of 2E1, and there are two Arg residues in the vicinity of Tyr354 of 2B6. It is of

great interest to characterize the role of the tyrosine residues that are most critical for the inactivation of the catalytic activity of P450s to see if they do in fact play a role in reductase binding or electron transfer. To address this issue, the mutagenesis of Tyr354 in 2B6 and Tyr422/Tyr317 in 2E1 is currently underway.

Although PN is a strong one- and two-electron oxidant, it cannot react directly with tyrosine. Tyrosine nitration has been shown to proceed via a free radical mechanism involving the simultaneous formation of the tyrosyl and NO_2 radicals to form 3-nitrotyrosine (*3, 6, 47*). In addition, PN can react with heme proteins to form an oxoferryl porphyrin intermediate concomitant with NO_2 radical formation, followed by the formation of a tyrosyl radical during the process leading to the nitration of tyrosine (*42, 47–49*). A similar mechanism that occurs even more efficiently than in other heme and nonheme proteins has been shown to occur during the reaction of PN with some heme-thiolate proteins, such as $P450_{BM3}$, choloperoxidase, and $P450_{nor}$ (*50, 51*). It has been demonstrated that heme plays a role in catalyzing the nitration of Tyr385 and the inactivation of prostaglandin H_2 synthase-1 by PN, and a heme-catalyzed mechanism involving an oxo-ferryl intermediate was proposed (*42*). In the presence of *n*-octylamine, which acts as a ligand to the heme iron and prevents reaction of PN with heme, nitrotyrosine-containing peptides were not detectable in 2B6 and 2E1 treated with 150 μM PN (data not shown). However, at this time, the absolute requirement of heme for the formation of nitrotyrosine in mammalian P450s is unclear, Thus, the mechanism for nitrotyrosine formation by the reaction with PN is also still under debate (*3, 6, 42, 47–51*).

Our results have shown that exposure to PN modifies the prosthetic heme of 2B6 but not 2E1. Exposure to PN also damages the prosthetic heme of P450s 2B4, 3A4, and 3A5 (Lin, H., and Hollenberg, P. F., unpublished observations) but not 2B1 (*21*). Thus, it appears that the PN-mediated modification of heme is P450-specific and may depend on a variety of factors, such as the size of active site, the amino acid residues near the heme center, or the proximity of the heme to the surface of the protein. The absence of a protein radical in a cytochrome *c* variant, which is resistant to heme degradation by hydrogen peroxide, suggests the possibility that the formation of a protein radical is necessary for the heme degradation process (*52*). However, this conclusion may not extend to P450 enzymes. Whether the PN-mediated heme modification of 2B6 is due to direct oxidation of the heme by PN or whether it results from the formation of a protein radical by PN is not clear (*42, 52*).

In conclusion, the two human P450s 2B6 and 2E1 have been used as models to investigate the potential adverse effects of PN on P450 catalytic activity. Similar effects have been shown for other human P450s: 2C9, 2D6, 3A4, and 3A5 (Lin, H., and Hollenberg, P. F., unpublished results). 3-Nitrotyrosine residues have been detected immunochemically in various proteins in affected areas of patients with neurodegenerative disorders, cardiovascular diseases, and diabetes, indicating that PN is generated in the brain, heart, liver, and other tissues and that it may be associated with major human diseases (*2–5*). P450s 2B6 and 2E1 are distributed in various regions of the brain, heart, and liver and metabolize a wide variety of drugs that act on the central nervous system, including alcohol and nicotine (*11–14*). Hence, under pathogenic conditions that generate PN, the metabolism of drugs and endogenous compounds may be altered by modifying P450s. The development of therapeutic agents to prevent the formation of nitrating agents such as PN may protect the P450 enzymes from inactivation.

Acknowledgment. This work was supported in part by NIH Grant CA16954 (to P.F.H) and VA Merit Grant 35533 (to L.W.). We are grateful to Drs. Ute M Kent and Yasushi Yoshigae for providing the purified P450 2E1 and for their valuable suggestions. We thank Dr. James R. Halpert (University of Texas Medical Branch, Galveston, TX) for his generous gift of the expression vectors for 2B6 and 2E1. We also thank Drs. Yoichi Osawa and Haoming Zhang for invaluable discussions.

Supporting Information Available: Results section describing the identification of Tyr244, Tyr268, and Tyr380 in 2B6 and Tyr69 and Tyr317 in 2E1 and Figures S1–S5 (including legends). This material is available free of charge via the Internet at http://pubs.acs.org.

References

(1) Beckman, J. S., and Koppenol, W. H. (1996) Nitric oxide, superoxide, and peroxynitrite: the good, the bad, and the ugly. *Am. J. Physiol. 271*, C1424–C1437.
(2) Ischiropoulos, H. (1998) Biological tyrosine nitration: a pathophysiological function of nitric oxide and reactive oxygen species. *Arch. Biochem. Biophys. 356*, 1–11.
(3) Radi, R., Peluffo, G., Alvarez, M. N., Naviliat, M., and Cayota, A. (2001) Unraveling peroxynitrite formation in biological systems. *Free Radical Biol. Med. 30*, 463–488.
(4) Greenacre, S. A. B., and Ischiropoulos, H. (2001) Tyrosine nitration: localizsation, quantification, consequences for protein function and signal transduction. *Free Radical Biol. Med. 34*, 541–581.
(5) Turko, I. V., and Murad, F. (2002) Protein nitration in cardiovascular diseases. *Pharmacol. Rev. 54*, 619–634.
(6) Radi, R. (2004) Nitric oxide, oxidants, and protein tyrosine nitration. *Proc. Natl. Acad. Sci. U.S.A. 101*, 4003–4008.
(7) Morgan, E. T. (1997) Regulation of cytochrome P450 during inflammation and infection. *Drug Metab. Rev. 29*, 1129–1188.
(8) Morgan, E. T. (2001) Regulation of cytochrome P450 by inflammatory mediators: why and how? *Drug Metab. Dispos. 29*, 207–212.
(9) Morgan, E. T., Ullrich, V., Daiber, A., Schmidt, P., Takaya, N., Shoun, H., Mcgiff, J. C., Oyekan, A., Hanke, C. J., Campbell, W. B., Park, C., Kang, J., Yi, H., Cha, Y., Mansuy, D., and Boucher, J. (2001) Cytochrome P450 and flavin monooxygenases targets and sources of nitric oxide. *Drug Metab. Dispos. 29*, 1366–1376.
(10) Fradette, C., Yamaguchi, N., and du Souich, P. (2004) 5 Hydroxytrpytamine is biotransformed by CYP2C9, 2C19 and 2B6 to hydroxylamine, which is converted into nitric oxide. *Br. J. Pharmacol. 141*, 407–414.
(11) Thum, T., and Borlak, J. (2000) Gene expression in distinct regions of the heart. *Lancet 355*, 979–983.
(12) Miksys, S., and Tyndale, R. F. (2004) The unique regulation of brain cytochrome P4502 (CYP2) family enzymes by drug and genetics. *Drug Metab. Rev. 36*, 313–333.
(13) Turpeinen, M., Raunio, H., and Pelkonen, O. (2006) The functional role of CYP2B6 in human drug metabolism: substrates and inhibitors in vitro, in vivo and in silico. *Curr. Drug Metab. 7*, 705–714.
(14) Spatzenegger, M., Liu, H., Wang, Q., Debarber, A., Koop, D. R., and Halpert, J. R. (2003) Analysis of differential substrate selectivities of CYP2B6 and CYP2E1 by site-directed mutagenesis and molecular modeling. *J. Pharmacol. Exp. Ther. 304*, 477–487.
(15) Crow, J. P., Ye, Y. Z., Strong, M., Kirk, M., Barnes, S., and Beckman, J. S. (1997) Superoxide dismutase catalyzes nitration of tyrosines by peroxynitrite in the rod and head domains of neurofilament-L. *J. Neurochem. 69*, 1945–1953.
(16) Souza, J. M., Daikhin, E., Yudkoff, M., Raman, C. S., and Ischiropoulos, H. 1999 Factors determining the selectivity of protein tyrosine nitration. *Arch. Biochem. Biophys. 371*, 169–178.
(17) Greis, K. D., Zhu, S., and Matalon, S. (1996) Identification of nitration sites on surfactant protein A by tandem electrospray mass spectrometry. *Arch. Biochem. Biophys. 335*, 396–402.
(18) MacMillan-Crow, L.A., Crow, J. P., and Thompson, J. A. (1998) Peroxynitrite-mediated inactivation of manganese superoxide dismutase involves nitration and oxidation of critical tyrosine residues. *Biochemistry 37*, 1613–1622.
(19) Han, D., Canali, R., Garcia, J., Aguilera, R., Gallaher, T. K., and Cadenas, E. (2005) Sites and mechanisms of aconitase inactivation by peroxynitrite: modulation by citrate and glutathione. *Biochemistry 44*, 11986–11996.
(20) Webster, R. P., Macha, S., Brockman, D., and Myatt, L. (2006) Peroxynitrite treatment in vitro disables catalytic activity of recombinant p38 MAPK. *Proteomics 6*, 4838–4844.

(21) Roberts, E. S., Lin, H., Crowley, J. R., Vuletich, J. L., Osawa, Y., and Hollenberg, P. F. (1998) Peroxynitrite-mediated nitration of tyrosine and inactivation of the catalytic activity of cytochrome P450 2B1. *Chem. Res. Toxicol. 11*, 1067–1074.
(22) Lin, H., Kent, U. M., Zhang, H., Waskell, L., and Hollenberg, P. F. (2003) Mutation of tyrosine 190 to Alaline eliminates the inactivation of cytochrome P450 2B1 by peroxynitrite. *Chem. Res. Toxicol. 16*, 129–136.
(23) Hanna, I. M., Teiber, J. F., Kokones, K. L., and Hollenberg, P. F. (1998) Role of alanine at position 363 of cytochrome P450 2B2 in influencing the NADPH- and hydroperoxide-supported activities. *Arch. Biochem. Biophys. 350*, 324–332.
(24) Omura, T., and Sato, R. (1964) The carbon monoxide-binding pigment of liver microsomes. I. Evidence for its hemoprotein nature. *J. Biol. Chem. 239*, 2370–2378.
(25) Guex, N., and Peitsch, M. C. (1997) SWISS-MODEL and the Swiss-PdbViewer: an environment for comparative protein modeling. *Electrophoresis 18*, 2714–2723.
(26) Thompson, J. D., Higgins, D. G., and Gibson, T. J. (1994) CLUSTAL W: improving the sensitivity of progressive multiple sequence alignment through sequence weighting, position-specific gap penalties and weight matrix choice. *Nucleic Acids Res. 22*, 4673–4680.
(27) Scott, E. E., White, M. A., He, Y. A., Johnson, E. F., Stout, C. D., and Halpert, J. R. (2004) Structure of mammalian cytochrome P4502B4 complexed with 4-(4-chlorophenyl)imidazole at 1.9-Å resolution. *J. Biol. Chem. 279*, 27294–27301.
(28) Sevrioukova, I. F., Li, H., Zhang, H., Peterson, J. A., and Poulos, T. L. (1999) Structure of a cytochrome P450-redox partner electron-transfer complex. *Proc. Natl. Acad. Sci. U.S.A. 96*, 1863–1868.
(29) Nicolis, S., Pennati, A., Perani, E., Monzani, E., Sanangelantoni, A. M., and Casella, L. (2006) Easy oxidation and nitration of human myoglobin by nitrite and hydrogen peroxide. *Chem.—Eur. J. 12*, 749–757.
(30) Bondoc, L. L., and Timkovich, R. (1989) Structural characterization of nitrimyoglobin. *J. Biol. Chem. 264*, 6134–6145.
(31) Sarver, A., Scheffler, K., Shetlar, M. D., and Bradford, W. G. (2001) Analysis of peptides and proteins containing nitrotyrosine by matrix-assisted laser desorption/ionization mass spectrometry. *Am. Soc. Mass Spectrom. 12*, 439–448.
(32) Petersson, A., Steen, H., Kalume, D. E., Caidahl, K., and Roepstorff, P. (2001) Investigation of tyrosine nitration in proteins by mass spectrometry. *J. Mass Spectrom. 36*, 616–625.
(33) Schmidt, P., Youhnovski, N., Daiber, A., Balan, A., Arsic, M., Bachschmid, M., Przybylski, M., and Ullrich, V. (2003) Specific Nitration at tyrosine 430 revealed by high resolution mass spectrometry as basis for redox regulation of bovine prostacyclin. *J. Biol. Chem. 278*, 12813–12819.
(34) Ortiz de Montellano, P. R., Ed. (1995) Oxygen Activation and Reactivity. In *Cytochrome P450: Structure, Mechanism, and Biochemistry*, pp 245–303, Plenum Press, New York.
(35) Roberts, E. S., Ballou, D. P., Hopkins, N. E., Alworth, W. L., and Hollenberg, P. F. (1995) Mechanistic studies of 9-ethynylphenanthrene-inactivataed cytochrome P450 2B1. *Arch. Biochem. Biophys. 323*, 303–312.
(36) Bridges, A., Gruenke, L., Chang, Y., vakser, I. A., Loew, G., and Waskell, L. (1998) Identification of the binding site on cytochrome P450 2B4 for cytochrome b_5 and cytochrome P450 reductase. *J. Biol. Chem. 273*, 17036–17049.
(37) Smallwood, H. S., Galeva, N. A., Bartlett, R. K., Urbauer, R. J. B., William, T. D., Urbauer, J. L., and Squier, T. C. (2003) Selective Nitration of Tyr99 in calmodulin as a marker of cellular conditions of oxidative stress. *Chem. Res. Toxicol. 16*, 95–102.
(38) Ischiropoulos, H., Zhu, L., Chen, J., Tsai, M., Martin, J. C., Smith, C. D., and Beckman, J. S. (1992) Peroxynitrite-mediated tyrosine nitration catalyzed by superoxide dismutase. *Arch. Biochem. Biophys. 298*, 431–437.
(39) Yamakura, F., Taka, H., Fujimura, T., and Murayama, K. (1998) Inactivation of human manganese-superoxide dismutase by peroxynitrite is caused by exclusive nitration of tyrosine 34 to 3-nitrotyrosine. *J. Biol. Chem. 273*, 14805–14089.
(40) Blanchard-Fillion, B., Souza, J. M., Friel, T., Jiang, G. C. T., Vrana, K., Sharov, V., Barron, L., Schoneich, C., Quijano, C., Alvarez, B., Radi, R., Przedborski, S., Fernando, G. S., Horwitz, J., and Ischiropoulos, H. 2001 Nitration and inactivation of tyrosine hydroxylase by peroxynitrite. *J. Biol. Chem. 273*, 46107–46023.
(41) Shimokawa, T., Kulmacz, R. J., DeWitt, D. L., and Smith, W. L. (1990) Tyrosine 385 of prostaglandin endoperoxide synthase is required for cyclooxygenase catalysis. *J. Biol. Chem. 265*, 20073–20076.
(42) Deeb, R. S., Hao, G., Gross, S. S., Laine, M., Qiu, J. H., Resnick, B., Barbar, E. J., Hajjar, D. P., and Upmacis, R. K. (2006) Heme catalyzes tyrosine 385 nitration and inactivation of prostaglandin H_2 synthase-1 by peroxynitrite. *J. Lipid Res. 47*, 498–911.
(43) Zhang, H., Myshkin, E., and Waskell, L. (2005) Role of cytochrome b_5 in catalysis by cytochrome P450 2B4. *Biochem. Biophys. Res. Commun. 338*, 499–506.
(44) Janig, G. R., Kraft, R., Rabe, H., Makower, A., and Ruckpaul, K. (1988) Comparative studies on the accessibility and functional importance of tyrosine residues in cytochrome P450 isozymes. *Biomed. Biochim. Acta 47*, 565–579.
(45) Bernhardt, R., Kraft, R., Otto, K. A., and Ruckpaul, K. (1988) Electrostatic interactions between cytochrome P450 LM2 and NADPH-cytochrome P450 reductase. *Biomed. Biochim. Acta 47*, 581–592.
(46) Sebban-Kreuzer, C., Blackledge, M., Dolla, A., Marion, D., and Guerlesquin, F. (1998) Tyrosine 64 of cytochrome c553 is required for electron exchange with formate dehydrogenase in Desulfovibrio vulgaris. *Biochemistry 37*, 8331–8340.
(47) Floris, R., Piersma, S. R., Yang, G., Jones, P., and Wever, R. (1993) Interaction of myeloperoxidase with peroxynitrite: a comparison with lactoperoxidase, horseradish peroxide and catalase. *Eur. J. Biochem. 215*, 767–775.
(48) Pietraforte, D., Salzano, A. M., Scorza, G., Marino, G., and Minetti, M. (2001) Mechanism of peroxynitrite interaction with ferric hemoglobin and identification of nitrated tyrosine residues: CO_2 inhibits heme-catalyzed scavenging and isomerization. *Biochemistry 40*, 15300–15309.
(49) Romero, N., Radi, R., Linares, E., Augusto, O., Detweiler, C. D., Manson, R. P., and Denicola, A. (2003) Reaction of human hemoglobin with peroxynitrite: isomerization to nitrate and secondary formation of protein radicals. *J. Biol. Chem. 278*, 44049–44057.
(50) Daiber, A., and Ullrich, V. (2002) Peroxynitrite reactions with heme and heme-thiolate (P450) proteins. *Methods Enzymol. 359*, 379–389.
(51) Daiber, A., Bachschmid, M., Munzel, T., and Ullrich, V. (2004) The impact of metal catalysis on protein tyrosine nitration by peroxynitrite. *Biochem. Biophys. Res. Commun. 317*, 873–881.
(52) Villegas, J. A., Mauk, A. G., and Vazquez-Duhalt, R. (2000) A cytochrome c variant resistant to heme degradation by hydrogen peroxide. *Chem. Biol. 7*, 237–244.

TX700220E